PHYSICAL REVIEW B VOLUME 15, NUMBER 3 1 FEBRUARY 1977

Polarized neutron study of ferromagnetic Ni-Cu alloys: Evidence for a magnetic environment effect*

R. A. Medina† and J. W. Cable
Solid State Division, Oak Ridge National Laboratory, Oak Ridge, Tennessee 37830

(Received 21 July 1976)

We measured the magnetic diffuse scattering of polarized neutrons from ferromagnetic Ni-Cu alloys with 19.8-, 29.6-, and 52.5-at.% Cu at 4.2 K. The data show that the Cu atoms are not polarized and that the negative polarization exists only around the Ni sites. Assuming that the Ni moments are a function of the moments of the neighboring atoms, we obtain an analytical expression for the polarized neutron cross section which describes the data well. This magnetic environment model is also shown to reproduce the moment disturbances of other dilute Ni based alloys. A Stoner type of calculation shows that between 20% and 40% interatomic exchange is needed to reproduce the Ni-Cu magnetization and cross sections; within the same calculation each Cu atom induces a (1–2)% moment reduction on its Ni neighbors for any given exchange field.

I. INTRODUCTION

The diffuse scattering of unpolarized neutrons was used by Cable *et al.*[1] and by Aldred *et al.*[2] to determine the moment disturbances in different ferromagnetic Ni-Cu alloys. The analysis of the data with the linear-superposition model proposed by Marshall[3] yielded a copper-cell average moment of $-0.1\ \mu_B$ constant over the range 0–40-at.% Cu. This is a very surprising result because any simple theory predicts approximate scaling with the bulk-average moment, which changes from 0.616 to 0.166 μ_B in the same range. Because of the negative uniform polarization observed in pure nickel,[4] and the experimental[5,6] and theoretical[7,8] evidence showing that the Cu keep its 3*d* shell full, the negative moment observed in the copper cells was identified with a uniform conduction-band polarization. This is, however, inconsistent with the more recent diffraction data[9] which show that the uniform polarization is instead roughly proportional to the bulk moment. This discrepancy was attributed in Ref. 9 to the nonlinearities neglected in the Marshall model, nonlinearities that Aldred *et al.* themselves considered very important and that Garland and Gonis[10] have estimated to be important for concentrations larger than 20-at.% Cu.

In view of this, we measured the moment disturbances of three Ni-Cu alloys (19.8-, 29.6-, and 52.5-at.% Cu) with the diffuse scattering of polarized neutrons; a method which gives directly the average moment $\langle \mu_{\mathrm{Cu}} \rangle - \langle \mu_{\mathrm{Ni}} \rangle$ without any model assumption. We also present a magnetic-environment model to interpret the results.

II. CROSS SECTIONS AND EXACT RELATIONS

The disorder diffuse scattering of polarized neutrons from a ferromagnetic substitutional binary alloy, such as Ni-Cu, is composed of three kinds of processes: the nuclear scattering, the magnetic scattering, and the spin-dependent nuclear-magnetic interference scattering. For neutrons polarized parallel ($\epsilon = 1$) or antiparallel ($\epsilon = -1$) to the magnetization, the cross section per atom may be written

$$\left(\frac{d\sigma}{d\Omega}\right)_\epsilon = \left(\frac{d\sigma}{d\Omega}\right)_N + \epsilon\left(\frac{d\sigma}{d\Omega}\right)_{NM} + \left(\frac{d\sigma}{d\Omega}\right)_M . \tag{2.1}$$

By measuring the cross sections for both polarizations and taking their difference, the interference term can be extracted. We have

$$\Delta \frac{d\sigma}{d\Omega} = 2\left(\frac{d\sigma}{d\Omega}\right)_{NM} \tag{2.2}$$

and

$$\sum_\epsilon \left(\frac{d\sigma}{d\Omega}\right)_\epsilon = 2\left(\frac{d\sigma}{d\Omega}\right)_N + 2\left(\frac{d\sigma}{d\Omega}\right)_M . \tag{2.3}$$

The diffuse nuclear scattering is proportional to the Fourier transform of the Cowley short-range-order (SRO) parameters. More precisely, if c is the impurity concentration, $p_{\vec{\mathrm{m}}}$ is the number of impurities at site $\vec{\mathrm{m}}$ ($p_{\vec{\mathrm{m}}} = 0, 1$), and $\langle\ \ \rangle$ is the configurational average, then the SRO parameters are defined as

$$c(1-c)\,\alpha(\vec{\mathrm{m}}) = \langle (p_{\vec{\mathrm{m}}+\vec{\mathrm{r}}} - c)(p_{\vec{\mathrm{r}}} - c)\rangle . \tag{2.4}$$

The nuclear-scattering cross section is then given by

$$\left(\frac{d\sigma}{d\Omega}\right)_N = c(1-c)(\Delta b)^2 S(\vec{\mathrm{K}}), \tag{2.5}$$

where Δb is the difference of impurity and host nuclear-scattering amplitudes

$$\Delta b = b_i - b_h \tag{2.6}$$

and $S(\vec{K})$ is the SRO scattering function

$$S(\vec{K}) = \sum_{\vec{m}} e^{i\vec{K}\cdot\vec{m}} \alpha(\vec{m}). \tag{2.7}$$

If the magnetization is perpendicular to the scattering plane, the magnetic cross section (in barns) is given by

$$\left(\frac{d\sigma}{d\Omega}\right)_M = c(1-c)\,\mathcal{T}(\vec{K})(0.270)^2. \tag{2.8}$$

Here, $\mathcal{T}(\vec{K})$ is a moment-moment correlation expressed in terms of $\mu_{\vec{n}}$ and $f_{\vec{n}}(\vec{K})$, the magnetic moment of the atom at site $\vec{n}$ and its form factor, respectively,

$$\mu_{\vec{n}}(\vec{K}) = \mu_{\vec{n}} f_{\vec{n}}(\vec{K}), \tag{2.9}$$

$$(1-c)c\,\mathcal{T}(\vec{K}) = \sum_{\vec{n}} e^{i\vec{K}\cdot\vec{n}} \langle \mu_{\vec{n}+\vec{r}}(\vec{K})[\mu_{\vec{r}}(\vec{K}) - \langle\mu(\vec{K})\rangle]\rangle. \tag{2.10}$$

Finally, the nuclear-magnetic interference term is proportional to a site-occupation–magnetic-moment correlation. For a magnetization perpendicular to the scattering plane, we have

$$\left(\frac{d\sigma}{d\Omega}\right)_{NM} = \tfrac{1}{2}\Delta\frac{d\sigma}{d\Omega} = c(1-c)\Delta b(0.540)\mathfrak{M}(\vec{K}) \tag{2.11}$$

and

$$c(1-c)\mathfrak{M}(\vec{K}) = \sum_{\vec{n}} e^{i\vec{K}\cdot\vec{n}} \langle (p_{\vec{n}+\vec{t}} - c)\mu_{\vec{t}}(\vec{K})\rangle, \tag{2.12}$$

where the quantity in angular brackets divided by c represents the average increase in the moment of the atom at site $\vec{t}$ when an impurity is located at site $\vec{n}+\vec{t}$.

The measurements performed on a polycrystalline sample give spherically averaged cross sections. The spherical average of $\mathfrak{M}(\vec{K})$, denoted (as any other spherical average) by dropping the vector symbol on K, complies with the following equation readily obtained from the definition (2.12):

$$\mathfrak{M}(K) = \langle\mu_i(K)\rangle - \langle\mu_h(K)\rangle + \cdots, \tag{2.13}$$

where the dots represent decaying oscillatory terms. Here $\langle\mu_i(K)\rangle$ and $\langle\mu_h(K)\rangle$ are the average impurity and host moments. We note that the large K values of $\mathfrak{M}(K)$ give directly the difference of average moments.

There is also an exact relationship between the concentration derivative of the average moment and the scattering in the forward direction[11]

$$\frac{d\langle\mu\rangle}{dc} = \frac{\mathfrak{M}(0)}{S(0)}. \tag{2.14}$$

Two hypotheses are assumed in the proof of (2.14). First, it is assumed that the moments are determined by their local environment, and second, that the samples used to measure the concentration derivative have suffered the same heat treatment. Finally, Marshall[3] gives a formula, valid within the linear superposition of perturbations, which is equivalent to the following equation:

$$\mathcal{T}(\vec{K}) \simeq \mathfrak{M}(\vec{K})^2/S(\vec{K}). \tag{2.15}$$

III. EXPERIMENTAL PROCEDURES AND CORRECTIONS

Three ferromagnetic samples of ^{62}Ni-Cu alloys with 19.8-, 29.6-, and 52.5-at.% Cu were used in these experiments. Two different chemical analyses of the last sample gave results of 53.5- and 52.5-at.% Cu. Our magnetization measurement on this sample $[(0.049 \pm 0.0025)\mu_B]$ is consistent with the second result.[12] The isotope ^{62}Ni was chosen because its negative scattering amplitude gives a large Δb. The isotopic composition of the enriched nickel was, in atomic %, ^{62}Ni 99.06%, ^{58}Ni 0.34%, ^{60}Ni 0.48%, ^{61}Ni 0.12%, and ^{59}Ni <0.05%. The main magnetic impurities present were Fe >0.001%, but <0.01%, and Mn <0.01%. Other impurities were Zn <0.2% and Th <0.2%. The nickel was combined with natural 99.995% copper.

The incoherent-scattering cross section of the nickel, and the copper-nickel scattering amplitude difference, calculated by taking into account the isotopic composition, are $\sigma_{\text{inc}}/4\pi = 0.0275 \pm 0.0002$ b and $\Delta b = (1.621 \pm .02) \times 10^{-12}$ cm.

The samples were polycrystalline plates about 1.5 mm thick. They were prepared by arc melting in a berylia crucible under an argon atmosphere, rolling the button to 70% of its thickness, annealing at 1050 °C for 16 h. and quenching. All neutron measurements were performed at 4.2 K. By the interpolation of published data,[13] we estimated the following 4.2-K lattice parameters: for the 20% sample, $a = 3.532$ Å; 30%, $a = 3.54$ Å; and 52.5%, $a = 3.56$ Å.

The experiments were carried out on the polarized-neutron spectrometer at the high-flux-isotope reactor at Oak Ridge National Laboratory. The incident beam had a wavelength of 1.067 Å and a polarization of 99%. The spectrometer was calibrated using a standard vanadium scatterer. The samples were mounted in symmetrical-transmission geometry with a vertical magnetic field. For the 20% and 30% samples, a field of 25 kOe was used, while measurements at 10 and 57 kOe were taken for the 52.5% alloy. A triple-axis arrangement with a Be analyzer in the zero-energy transfer position was used for the smaller angles (<2.5°) in order to avoid the main beam. These small-angle measurements were calibrated by comparison between the two arrangements in an overlap region (2.5°–3.5°).

The scattering of both neutron polarizations, parallel and antiparallel to the magnetic field, was measured inside the first Bragg peak. The sum and the difference of the cross sections of the two spin states were calculated, taking into account the instrumental background and the polarization of the beam. No beam depolarization by the samples was observed.

The following processes contribute to the scattering: (i) disorder diffuse scattering, nuclear and magnetic, as explained in Sec. II, (ii) incoherent scattering, (iii) multiple scattering, (iv) thermal diffuse scattering. This last contribution is negligible at the temperatures and wave vectors of these experiments. The incoherent scattering is spin independent and therefore contributes only to the sum cross section. This contribution was calculated and then subtracted. The multiple scattering for both spin states was also estimated and subtracted. We used the standard method[14] which requires measurement of the spin-dependent transmission.

The expression given in Sec. II for the difference cross section assumes that the magnetization is perpendicular to the scattering vector, e.g., it is valid only for perfect vertical resolution. In a more general case, the measured cross section is

$$\left(\Delta \frac{d\sigma}{d\Omega}(K)\right)_{\text{meas}} = \int_{-\infty}^{\infty} \frac{K^2}{K^2+W^2} \frac{e^{-(W/\eta)^2}}{\eta\sqrt{\pi}} \times \Delta \frac{d\sigma}{d\Omega} (K^2+W^2)^{1/2}\, dW , \quad (3.1)$$

where K is the component of the scattering vector perpendicular to the magnetization, W is the parallel component, and a Gaussian vertical resolution of width $2(\ln 2)^{1/2}\eta$ is assumed. A direct measurement of η and a geometrical calculation lead to essentially the same value $\eta = 0.12$ Å^{-1}. The integral equation (3.1), which can be analytically inverted, was used to correct the difference cross section with the method of spline functions.[15] The correction was as large as 15% for the innermost points. The sum cross section, as previously explained, is composed of a nuclear and a magnetic term. The large value of Δb of the samples insures that the magnetic contribution is only a small fraction of the sum cross section. It is therefore a proper approximation to use Eq. (2.15) to calculate the magnetic term. We obtain from (2.3),

$$\sum_{\epsilon} \left(\frac{d\sigma}{d\Omega}\right)_{\epsilon} \simeq 2\left(\frac{d\sigma}{d\Omega}\right)_{N} + \frac{1}{8}\left(\Delta \frac{d\sigma}{d\Omega}\right)^{2} \Big/ \left(\frac{d\sigma}{d\Omega}\right)_{N} . \quad (3.2)$$

This equation was used to calculate the nuclear cross section.

IV. DIRECT RESULTS: MOMENT AND FORM FACTOR

In this section, we discuss the direct information that can be obtained from the measured cross sections. In particular, we consider the implications of Eqs. (2.13) and (2.14).

The Ni-Cu alloys exhibit substantial clustering that must be taken into account when considering the magnetic-moment distributions. We therefore must first obtain the SRO parameters from the data. This is accomplished by fitting the nuclear cross section with a function of the following form:

$$[c(1-c)(\Delta b)^2]^{-1} \left(\frac{d\sigma}{d\Omega}\right)_N = S(K) = \sum_{\lambda} \alpha(R_\lambda) Z_\lambda j_0(K R_\lambda). \quad (4.1)$$

Here Z_λ is the coordination number, and R_λ is the radius of the shell. Theoretically $\alpha(0) = 1$, but in the fitting we consider it as a free parameter to compensate for any possible error in the determination of the incoherent and multiple scattering that was subtracted to obtain the nuclear cross section. The results of the fittings are given in Table I and Fig. 1. For the 30% alloy, it was necessary to use up to nine shells in order to get a good fit with reasonably small SRO parameters; in this case the parameters were constrained to be small. Comparison of our results with those of Aldred *et al.*,[2] Cable *et al.*,[1] and Mozer *et al.*[16] shows that the SRO parameters of these samples are slightly larger than those previously reported. This is not surprising because the SRO may be sample dependent. There is also a difference in the sign of $\alpha(R_2)$ between our results and some of the previous results.[1,2] It should be noted that, because of the larger nuclear cross sections of our samples and/or the larger range in K values of our data, the present SRO results should be more accurate than those obtained in Refs. 1 and 2. Nevertheless, all of the SRO measurements indicate that clustering is present in these alloys.

An important result that can be obtained from the data is the solution of the apparent discrepancy between the diffraction data and the unpolarized-neutron diffuse-scattering data. The Bragg scattering results for pure Ni by Mook,[4] and for Ni-Cu by Ito and Akimitsu[9] show that the *average* moment density is composed of a local atomic-like moment density and a uniform negative magnetization between sites. The Ito and Akimitsu

TABLE I. SRO parameters.

c	α_0	α_1	α_2	α_3	α_4	α_5	α_6	α_7	α_8	α_9	χ^2/N
0.198	1.006 (4)	0.1175 (35)	−0.0614	0.0445	−0.0584	0.0263					1.3
0.296	0.950 (9)	0.1432 (82)	−0.0328	0.0432	−0.0098	0.0108	0.0225	0.0037	−0.0211	0.0065	0.97
0.525	0.890 (3)	0.1335 (33)	−0.0747	0.0436	−0.0479	0.0148					0.80

data indicate that the uniform magnetization decreases monotonically with increasing Cu content and is roughly proportional to the local moment. On the other hand, the unpolarized-neutron experiments[1,2] were interpreted to imply the existence of a uniform moment and/or local Cu moment totaling $-0.1\,\mu_B$ over the range 0–40-at.% Cu. The moment values that we obtain from our polarized-neutron data, which are more easily analyzed, are not in contradiction with the diffraction data.

In previous analyses of diffuse-scattering data,[1,2] it has been assumed that the negative magnetization not seen in diffraction experiments is truly uniform, and therefore, unobservable even by diffuse-scattering experiments. Consequently, a local atomic or ionic form factor was assigned to all observed moments. If this assumption were true, the quantity $\mathfrak{M}(0)/S(0)$ should be equal to the concentration derivative of the *local* moment, now known to be approximately $-1.35\mu_B$. To the contrary, our polarized-neutron scattering data clearly show that $\mathfrak{M}(0)/S(0)$ is equal to the concentration derivative of the *bulk* moment (see Table II). This confirms the theoretical argument made elsewhere[17] that the negative magnetization in alloys consists only of short-range contributions from each magnetic atom. Its form factor, although negligible at Bragg peaks, can be seen by diffuse neutron scattering. This result was suggested only ambiguously by the analysis of the earlier unpolarized-neutron scattering data.[1,2]

The negative magnetization was originally attributed to s-p band polarization. On the other hand, Moon[18] has suggested that it is part of the d-electron moment. As explained in detail elsewhere,[17] both suggestions lead to very similar form factors. We have followed Moon's assumption, and use a Ni form factor of the form

$$\langle f(K)\rangle = [1+0.154(1-c)]f_l(K) - 0.154(1-c)f_{\text{ov}}(K), \qquad (4.2)$$

where $f_{\text{ov}}(K)$ is the spherically averaged "overlap" form factor to be associated with the negative polarization (see Fig. 2), and $f_l(K)$ is the form factor of the local moment. Both $f_l(K)$ and the constant 0.154 were chosen to be consistent with the diffraction data. The factor $(1-c)$ appears because we assume that there is no "overlap" between $3d$ electrons of Ni and Cu atoms. For the analysis of the moment disturbances, we neglect the difference between the Ni and Cu form factors. This introduces no error because the Cu moment is negligible.

The nuclear-magnetic interference cross section has been fitted with an expression of the following form obtained by taking the spherical average of (2.12):

$$\frac{\mathfrak{M}(K)}{\langle f(K)\rangle} = \sum_{\lambda} Z_\lambda m_\lambda j_0(KR_\lambda). \qquad (4.3)$$

Here Z_λ and R_λ keep the meaning they have in Eq. (4.1), while the m_λ are the moment disturbances. The fitted values of $m_0 = \Delta\langle\mu\rangle = \langle\mu_{\text{Cu}}\rangle - \langle\mu_{\text{Ni}}\rangle$ are shown in Table II. For comparison, values of $\langle\mu\rangle/(1-c)$ are also given. The agreement between these two quantities indicates that the Cu moment is essentially zero, as the calculated values in the last column of Table II confirm. The low-field value of $\langle\mu\rangle$ for the 52.5% alloy was measured by us. All the other values of $\langle\mu\rangle$ and those of $d\langle\mu\rangle/dc$ were obtained from

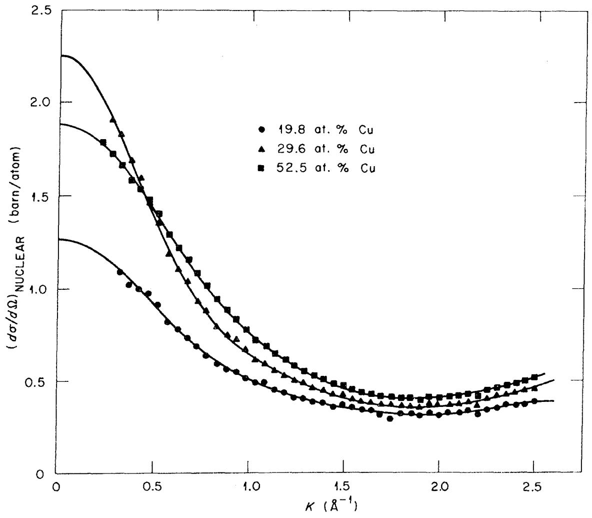

FIG. 1. Nuclear diffuse-scattering cross sections of Ni-Cu alloys.

TABLE II. Magnetic moments and concentration derivatives for Ni–Cu alloys.

c	H(kOe)	$\langle\mu_{\mathrm{Ni}}\rangle - \langle\mu_{\mathrm{Cu}}\rangle$ [a]	$\langle\mu\rangle/(1-c)$	$\mathfrak{M}(0)/S(0)$	$d\langle\mu\rangle/dc$	$\langle\mu_{\mathrm{Cu}}\rangle$
0.198	25	0.478 (5)	0.486 (3)	−1.125 (10)	−1.140 (10)	0.006 (13)
0.296	25	0.413 (6)	0.397 (6)	−1.128 (10)	−1.120 (10)	−0.011 (12)
0.525	10	0.091 (2)	0.103 (5)	−0.65 (2)	−0.66 (2)	0.006 (7)
0.525	57	0.106 (2)	0.114 (6)	−0.72 (2)	−0.79 (6)	0.004 (7)

[a] Multiple-scattering uncertainty of 0.015 μ_B must be added the statistical error quoted.

published magnetization data.[2,9,19-23] The tabulated values of $\mathfrak{M}(0)/S(0)$ were obtained by fitting $\mathfrak{M}(K)/[\langle f(K)\rangle S(K)]$ to an expression similar to (4.3). Both fittings and the data are shown in Fig. 3 where the arrows indicate the values of $d\langle\mu\rangle/dc$. Our values of $-\Delta\langle\mu\rangle$ are smaller than those obtained from the unpolarized-neutron experiments. For example, at 20% Cu we obtain $\Delta\langle\mu\rangle = -0.478\ \mu_B$ compared with the previous result[1,2] of $-0.60\ \mu_B$. We attribute this discrepancy mainly to the previous authors having neglected the difference between the spherical average of a product and the product of the spherical averages in Marshall's expression for the cross section [equivalent to our Eq. (5.9) or (2.15)]. This approximation is correct at small K, but wrong for the large K values that are important in determining $\Delta\langle\mu\rangle$. We calculate that, for the 20% data of Ref. 1, half of the discrepancy comes from this approximation. The remaining difference may arise from the different form factor assumptions used and from the nonlinear contributions to the unpolarized-neutron cross section.

To sum up this section, the magnetic moments in Ni-Cu, including the "uniform" negative magnetization, are associated with nickel atoms and there is no contradiction between the diffuse scattering and the diffraction data.

V. MANY-SITE PERTURBATIONS EXPANSION

In order to develop the magnetic-environment model of the next section, we need a many-site perturbation expansion, in which the moment on an atom is expanded as the average moment, plus the linear superposition of perturbations produced by the kind of occupation of single sites, plus the extra perturbation produced by pairs of sites, plus the n-site perturbations. This procedure is particularly useful if the perturbations are small, so that the many-site perturbations are increasingly negligible. One of the advantages of this description is that it allows for a simple treatment of the effects of short range order. The formulas we quote here are extensions of those given by Marshall[3] and by Balcar and Marshall.[24] We may write for the *random alloy*

$$\begin{aligned}\mu_{\vec{m}}(\vec{K}) = \bar{\mu}(\vec{K}) &+ \sum_{\vec{r}} \tilde{\phi}_1(\vec{K};\vec{r})(p_{\vec{m}+\vec{r}}-c)\\ &+ \frac{1}{2!}\sum_{\vec{r},\vec{t}} \tilde{\phi}_2(\vec{K};\vec{r},\vec{t})(p_{\vec{r}+\vec{m}}-c)(p_{\vec{t}+\vec{m}}-c)\\ &+ \frac{1}{3!}\sum_{\vec{r},\vec{t},\vec{n}} \tilde{\phi}_3(\vec{K};\vec{r},\vec{t},\vec{n})(p_{\vec{r}+\vec{m}}-c)\\ &\qquad\times(p_{\vec{t}+\vec{m}}-c)(p_{\vec{m}+\vec{n}}-c)+\cdots\,. \end{aligned} \tag{5.1}$$

The moment disturbances $\tilde{\phi}_\alpha(\vec{K};\vec{r}_1,\vec{r}_2,\ldots,\vec{r}_\alpha)$ are symmetric functions of the arguments $\vec{r}_\lambda$, and they vanish if any two of the arguments are equal. If we define

$$\tilde{\phi}_\alpha(\vec{K};\vec{r}_1,\ldots,\vec{r}_{\alpha-1}) = \sum_{\vec{m}} e^{i\vec{K}\cdot\vec{m}}\,\tilde{\phi}_\alpha(\vec{K};\vec{r}_1+\vec{m},\ldots,\vec{r}_{\alpha-1}+\vec{m},\vec{m}), \tag{5.2}$$

it is straightforward to prove that for the random alloy

$$\langle\mu(\vec{K})\rangle = \bar{\mu}(\vec{K}), \tag{5.3}$$

$$\mathfrak{M}(\vec{K}) = \tilde{\Phi}_1(\vec{K}), \tag{5.4}$$

and

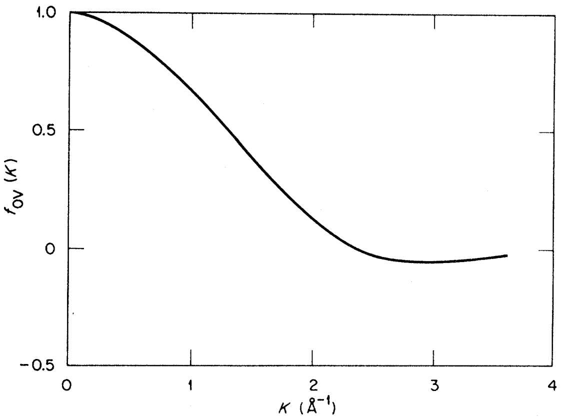

FIG. 2. Spherically averaged overlap form factor of Ni.

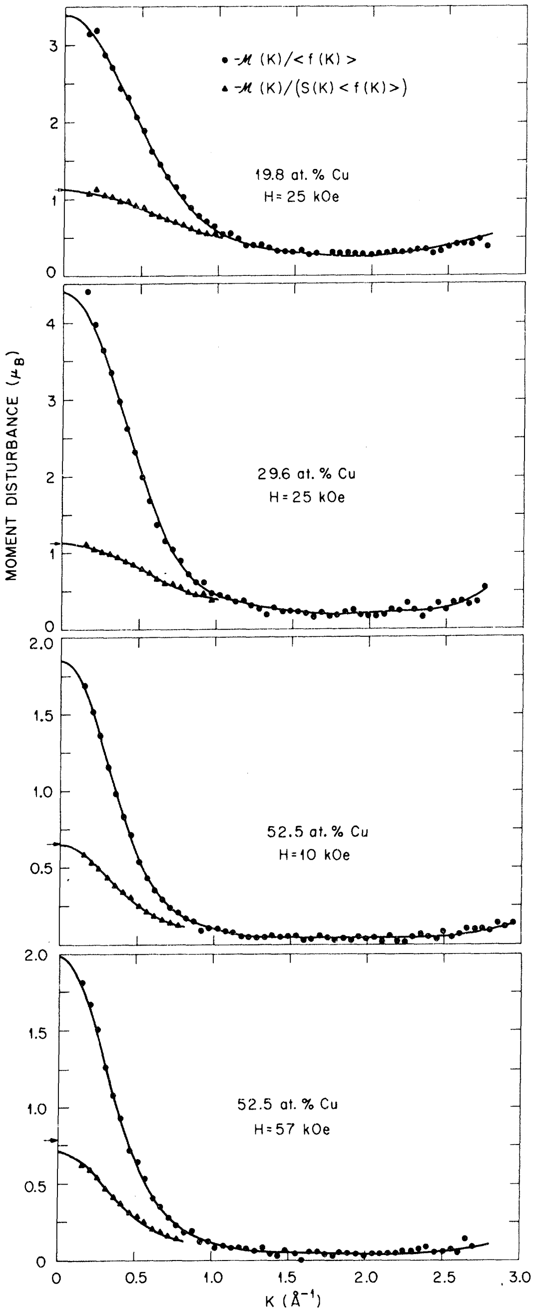

FIG. 3. Ni-Cu moment disturbances from diffuse scattering of polarized neutrons.

$$\mathcal{T}(\vec{K}) = |\tilde{\Phi}_1(\vec{K})|^2 + \frac{c(1-c)}{2!}\sum_{\vec{r}} |\tilde{\Phi}_2(\vec{K};\vec{r})|^2 + \frac{c^2(1-c)^2}{3!}\sum_{\vec{r},\vec{t}} |\tilde{\Phi}_3(\vec{K};\vec{r},\vec{t})|^2 + \cdots . \tag{5.5}$$

Note that for the random alloy the interference term in the cross section $\mathfrak{M}(K)$ contains only the single-site perturbations. Note also that, if the many-site perturbations are negligible, $\mathcal{T}(K)$ is just the square of $\mathfrak{M}(K)$. This relationship breaks down when the many-site perturbations are important; for example, we should expect this to happen near the critical composition of Ni-Cu.

When short-range order is present, we can still use the moment expansion (5.1) if we treat the introduction of SRO as a perturbation on the random alloy; this treatment may become inaccurate near the critical composition of Ni-Cu. The expansion is therefore done in terms of the parameters the alloy would have if it were random and the SRO introduced only into the processes of averaging. Following this path, we obtain to first order in the α's,

$$\langle \mu(\vec{K})\rangle = \bar{\mu}(\vec{K}) + \frac{c(1-c)}{2!}\sum_{\vec{r},\vec{t}} \tilde{\phi}_2(\vec{K};\vec{r},\vec{t})\alpha(\vec{r}-\vec{t}) + \cdots \tag{5.6}$$

and

$$\mathfrak{M}(\vec{K}) = S(\vec{K})[\tilde{\Phi}_1(\vec{K}) + (1-2c)V(\vec{K})] + \cdots , \tag{5.7}$$

where

$$V(\vec{K}) = \sum_{\vec{r},\vec{m}} \tilde{\Phi}_2(\vec{K},\vec{r},\vec{m})\alpha(\vec{r}-\vec{m})e^{i\vec{K}\cdot\vec{m}} . \tag{5.8}$$

The moment-moment correlation is given by

$$\mathcal{T}(\vec{K}) = S(\vec{K})[\tilde{\Phi}_1(\vec{K}) + (1-2c)V(\vec{K})]^2 + \text{terms in } (\tilde{\phi}_2)^2. \tag{5.9}$$

In the case of polycrystalline samples, the measurements give spherical averages. The analysis of this case is simplified when the difference among the form factors is neglected. In the Ni-Cu case, where $\mu_{Cu} = 0$, this approximation neglects only the environmental dependence of the form factor. We may write

$$\bar{\mu}(K) = \langle f(\vec{K})\rangle\, \bar{\mu}. \tag{5.10}$$

$$\tilde{\phi}_\alpha(\vec{K};\vec{r}_1,\ldots,\vec{r}_\alpha) = \langle f(\vec{K})\rangle\, \phi_\alpha(\vec{r}_1,\ldots,\vec{r}_\alpha). \tag{5.11}$$

Equation (5.7) then becomes

$$\mathfrak{M}(\vec{K}) = \langle f(\vec{K})\rangle\, S(\vec{K})\sum_{\vec{m}} \gamma(\vec{m})e^{i\vec{K}\cdot\vec{m}} , \tag{5.12}$$

where

$$\gamma(\vec{m}) = \phi_1(\vec{m}) + (1-2c)\sum_{\vec{m}} \phi_2(\vec{r},\vec{m})\alpha(\vec{r}-\vec{m}). \tag{5.13}$$

If we neglect the asphericity of $f(\vec{K})$, the spherical average is given by

$$\mathfrak{M}(K)\simeq\langle f(K)\rangle\sum_{\vec{m}}\gamma(\vec{m})\sum_{\vec{r}}\alpha(\vec{r})j_0(K|\vec{r}+\vec{m}|). \tag{5.14}$$

We use this equation to obtain the random-moment perturbation $\Phi_1(K)$ for comparison with the magnetic-environment model.

A simplified version of (5.13) is obtained when the two-site perturbations are small and the impurity moment is zero. In that case

$$\phi_2(\vec{r},\vec{m})\simeq-\frac{[\phi_1(\vec{r})\delta_{\vec{m}0}+\phi_1(\vec{m})\delta_{\vec{r}0}][1-\delta_{\vec{r}\vec{m}}]}{1-c} \tag{5.15}$$

and

$$\gamma(0)=\phi_1(0)-\frac{1-2c}{1-c}\sum_{\vec{r}\neq 0}\phi_1(\vec{r})\alpha(\vec{r}),$$

$$\gamma(\vec{m})=\phi_1(\vec{m})\left(1-\frac{1-2c}{1-c}\alpha(\vec{m})\right)\quad\text{for }\vec{m}\neq 0. \tag{5.16}$$

VI. MAGNETIC ENVIRONMENTAL MODEL

Chemical environment effects are expected to be small and short ranged for Ni-Cu. Nevertheless, the moment disturbances are long ranged for the concentrated alloys. This suggests that the moment of a nickel atom is a function not only of its nearest chemical environment, but also of the magnetic moments of the surrounding atoms. Different models incorporating this idea have been proposed.[10,25-29] In particular, Hicks[29] proposed a magnetic-environment model for Ni-Cu near the critical concentration which is very similar to the one developed here. Our model differs from Hicks in four aspects: (i) it does not assume a particular form for the response function, (ii) it is developed for the ferromagnetic instead of the critical region, (iii) it allows for a chemical environment effect, and (iv) we obtain a different analytical solution.

The proposed model is: The moment on a nickel atom is assumed to be a function of the number of Cu neighbors and of an effective exchange field produced by its neighbors. A random alloy is assumed. We then have

$$\mu_{\vec{m}}=(1-p_{\vec{m}})F(h(\vec{m}),\nu(\vec{m}),c), \tag{6.1}$$

in which h is the exchange field given by

$$h(\vec{n})=\sum_{\vec{m}}j(\vec{n}-\vec{m})\mu_{\vec{m}},\qquad j(0)=0, \tag{6.2}$$

and ν is the number of Cu next neighbors (a greek site index will stand for first neighbors)

$$\nu(\vec{m})=\sum_{\vec{\delta}}p_{\vec{m}+\vec{\delta}}. \tag{6.3}$$

The explicit concentration dependence of F takes into account the chemical environment beyond the first shell.

An approximate solution can be obtained if the equations are linearized in a way similar to that used by Lovesey and Marshall[30] in treating the temperature dependence of the cross section. If we assume that the fluctuations are small and that the chemical environment effect is small, we may write

$$F(h(\vec{n}),\nu(\vec{n}),c)\simeq F(h_{\text{eff}},\langle\nu\rangle,c)+\frac{\partial F}{\partial h}[h(\vec{n})-h_{\text{eff}}]+\frac{\partial F}{\partial\nu}[\nu(\vec{n})-\langle\nu\rangle], \tag{6.4}$$

where h_{eff} is an effective field defined as

$$\bar{\mu}_{\text{Ni}}=\bar{\mu}/(1-c)=F(h_{\text{eff}},\langle\nu\rangle,c). \tag{6.5}$$

By multiplying Eq. (6.4) by $(1-p_n)$ and taking the average, one obtains the following equation for the effective field:

$$\langle(1-p_{\vec{n}})[h(\vec{n})-h_{\text{eff}}]\rangle=0. \tag{6.6}$$

It is convenient now to introduce the many-site perturbations of the moment

$$\mu_{\vec{n}}=\bar{\mu}+\sum_{\vec{r}}\phi_1(\vec{r}-\vec{n})(p_{\vec{r}}-c)+\frac{1}{2}\sum_{\vec{r},\vec{t}}\phi_2(\vec{r}-\vec{n},\vec{t}-\vec{n})(p_{\vec{r}}-c)(p_{\vec{t}}-c)+\cdots. \tag{6.7}$$

Insertion of this into the definition of the exchange field gives

$$h(\vec{n})=\sum_{\vec{m}}j(\vec{n}-\vec{m})\mu_{\vec{m}}=\bar{\mu}\left(\sum_{\vec{r}}j(\vec{r})\right)+\sum_{\vec{r}}\sum_{\vec{m}}j(\vec{n}-\vec{m})\phi_1(\vec{r}-\vec{m})(p_{\vec{r}}-c)+\frac{1}{2}\sum_{\vec{r},\vec{t}}\left(\sum_{\vec{m}}j(\vec{n}-\vec{m})\phi_2(\vec{r}-\vec{m},\vec{t}-\vec{m})\right)\times(p_{\vec{r}}-c)(p_{\vec{t}}-c)+\cdots, \tag{6.8}$$

which, with (6.6), yields

$$h_{\mathrm{eff}}=\bar{\mu}\sum_{\vec{\mathrm{r}}} j(\vec{\mathrm{r}})-c\sum_{\vec{\mathrm{m}}} j(\vec{\mathrm{m}})\phi_1(\vec{\mathrm{m}}). \tag{6.9}$$

We now obtain an equation for the one-site perturbations $\phi_1(\vec{\mathrm{r}})$. From Eq. (6.7), it follows that

$$c(1-c)\phi_1(\vec{\mathrm{r}})=\langle(p_{\vec{\mathrm{r}}}-c)\mu_0\rangle, \tag{6.10}$$

from which we obtain $\phi_1(\vec{\mathrm{r}})$ by using the expression for the moment given by Eqs. (6.1) and (6.4), i.e.,

$$\phi_1(\vec{\mathrm{r}})=-\bar{\mu}_{\mathrm{Ni}}\,\delta_{\vec{\mathrm{r}}0}+\frac{\partial F}{\partial h}\left((1-c)(1-\delta_{\vec{\mathrm{r}}0})\sum_{\vec{\mathrm{m}}} j(-\vec{\mathrm{m}})\phi_1(\vec{\mathrm{r}}-\vec{\mathrm{m}})-c(1-c)\sum_{\vec{\mathrm{n}}} j(-\vec{\mathrm{n}})\phi_2(\vec{\mathrm{r}}-\vec{\mathrm{n}},-\vec{\mathrm{n}})\right)+\frac{\partial F}{\partial \nu}(1-c)\sum_{\vec{\rho}}\delta_{\vec{\rho}\vec{\mathrm{r}}}. \tag{6.11}$$

Note that ϕ_2 appears in this equation. In the same way, we can obtain an equation for ϕ_2 in which ϕ_3 appears. In general, an infinite set of equations can be obtained, each one relating the n-site perturbations with $(n+1)$-site perturbations. One way of solving the problem is to neglect the $(n+1)$-site perturbations, and to solve the truncated system of equations. We limit ourselves here to the first equation of the infinite set, which means that we neglect the two-site perturbations. This is justified because the average moment decreases linearly with concentration in the region 0–45-at.% Cu, and because the relation (2.15) between polarized- and unpolarized-neutron cross sections is roughly satisfied for Ni-Cu. Furthermore, when the two-site perturbations are included, the polarized-neutron cross section $\Phi_1(K)$ has approximately the same mathematical form of the cross section obtained taking only the one-site perturbations. Only the values of the parameters are different. We then drop the two-site perturbations and Fourier transform Eq. (6.11) to obtain

$$\Phi_1(\vec{\mathrm{K}})=-\left(\bar{\mu}_{\mathrm{Ni}}+\Gamma\sum_{\vec{\mathrm{n}}}\frac{j(\vec{\mathrm{n}})\phi_1(\vec{\mathrm{n}})}{J(0)}-\Gamma Z_1\rho F_1(\vec{\mathrm{K}})\right)\Big/\left(1-\frac{\Gamma J(\vec{\mathrm{K}})}{J(0)}\right). \tag{6.12}$$

Here J and Φ_1 are the Fourier transforms of j and ϕ_1, respectively. We have also introduced

$$\Gamma=\frac{\partial F}{\partial h}(1-c)J(0), \tag{6.13}$$

$$\rho=\frac{\partial F}{\partial \nu}\frac{(1-c)}{\Gamma}, \tag{6.14}$$

and

$$F_1(\vec{\mathrm{K}})=\frac{1}{Z_1}\sum_{\vec{\delta}} e^{i\vec{\mathrm{K}}\cdot\vec{\delta}}. \tag{6.15}$$

The parameter Γ is related to the range of the one-site perturbations, while ρ measures the strength of the chemical environment effect. The quantity

$$\sum_{\vec{\mathrm{n}}} j(\vec{\mathrm{n}})\phi_1(\vec{\mathrm{n}})$$

appearing in Eq. (6.12) is determined by Eq. (6.12) since

$$\sum_{\vec{\mathrm{n}}} j(\vec{\mathrm{n}})\phi_1(\vec{\mathrm{n}})=\frac{1}{V_{\mathrm{FBZ}}}\int_{\mathrm{FBZ}} d^3K\,J(\vec{\mathrm{K}})\Phi_1(\vec{\mathrm{K}}), \tag{6.16}$$

where the integral is over the first Brillouin zone. Using (6.16), we find

$$\frac{1}{J(0)}\sum_{\vec{\mathrm{n}}} j(\vec{\mathrm{n}})\phi_1(\vec{\mathrm{n}})=-\bar{\mu}_{\mathrm{Ni}}\frac{B(\Gamma)-1}{B(\Gamma)\Gamma}+\frac{\rho Z_1\tilde{B}(\Gamma)}{B(\Gamma)}, \tag{6.17}$$

where $B(\Gamma)$ and $\tilde{B}(\Gamma)$ are defined by

$$B(\Gamma)=\frac{1}{V_{\mathrm{FBZ}}}\int_{\mathrm{FBZ}} d^3K\frac{1}{1-\Gamma J(\vec{\mathrm{K}})/J(0)} \tag{6.18}$$

and

$$\tilde{B}(\Gamma)=\frac{1}{V_{\mathrm{FBZ}}}\int_{\mathrm{FBZ}} d^3K\frac{F_1(\vec{\mathrm{K}})}{1-\Gamma J(\vec{\mathrm{K}})/J(0)}. \tag{6.19}$$

The function $B(\Gamma)$ has the same form as a one-electron Green's function. Using (6.17) in (6.12) and (6.9), we find

$$\Phi_1(\vec{\mathrm{K}})=\frac{-\bar{\mu}_{\mathrm{Ni}}+Z_1\rho\Gamma[B(\Gamma)F_1(\vec{\mathrm{K}})-\tilde{B}(\Gamma)]}{B(\Gamma)[1-\Gamma J(\vec{\mathrm{K}})/J(0)]} \tag{6.20}$$

and

$$h_{\mathrm{eff}}=\bar{\mu}_{\mathrm{Ni}}J(0)\left((1-c)+c\frac{B(\Gamma)-1}{B(\Gamma)\Gamma}\right)-\frac{cJ(0)Z_1\rho\tilde{B}(\Gamma)}{B(\Gamma)}. \tag{6.21}$$

When ϕ_2 terms are included, $\Phi_1(\vec{\mathrm{K}})$ is still approximately given by Eq. (6.20) but with Γ replaced by a different value. We can then treat the effect of the neglected many-site perturbations by considering Γ as a parameter to be determined. Γ then assumes the value given by Eq. (6.13) only at zero-impurity concentration. The parameter Γ can be obtained self-consistently by imposing the equality of $\Phi_1(0)$ and the concentration derivative of the average moment

$$\frac{d\bar{\mu}}{dc}=\Phi_1(0). \tag{6.22}$$

This equation, together with (6.5), (6.14), (6.20), and (6.21), determined Γ and $\bar{\mu}$ as functions of concentration for any given $F(h, \nu, c)$.

In the particular case of nearest-neighbor exchange, the equations assume a simpler form. In this case

$$J(\vec{K}) = J(0)F_1(\vec{K}), \tag{6.23}$$

$$\tilde{B}(\Gamma) = [B(\Gamma) - 1]/\Gamma, \tag{6.24}$$

and Eq. (6.20) reduces to

$$\Phi_1(\vec{K}) = -\rho Z_1 - \frac{\bar{\mu}_{\mathrm{Ni}} - \rho Z_1}{[1 - \Gamma F_1(\vec{K})]B(\Gamma)}\,. \tag{6.25}$$

Furthermore, the function $B(\Gamma)$ has been calculated analytically[31] for nearest-neighbor exchange; the result is a combination of complete elliptic integrals.

VII. COMPARISON WITH DATA

A. Cross section

To compare the magnetic-environment model of Sec. VI with the diffuse-scattering data, we should extract from them the moment disturbances corresponding to the random alloy. This is done by fitting the data with Eq. (5.14) to obtain the parameters γ_λ. The one-site perturbations $\phi_1(R)$ are then calculated using these γ_λ in Eq. (5.16). As a check of this procedure, we have calculated the average Ni moment for the alloy with SRO, using Eq. (5.6). The comparison of these values with those obtained directly in Sec. III is given in Table III. The values for the random alloy $\bar{\mu}_{\mathrm{Ni}} = -\phi_1(0)$ are also listed. The magnetic-environment model gives a simple formula for $\Phi_1(\vec{K})$, but not for the coefficients $\phi_1(R)$. It is, therefore, more convenient to compare the model with a pseudoexperimental $\Phi_1(\vec{K})$ obtained from the $\mathfrak{M}(\vec{K})$ data by requiring that the percentage difference of the pseudodata and the calculated $\Phi_1(\vec{K})$ be equal to the percentage difference between the $\mathfrak{M}(\vec{K})$ data and their fitted values. The $\Phi_1(\vec{K})$ so obtained are shown in Fig. 4. The continuous lines in Fig. 4 represent the result of the fitting of the magnetic environment model with nearest-neighbor exchange [formula (6.25)] and give a good description of the data. The values of the free parameters $\bar{\mu}_{\mathrm{Ni}}$, Γ, and ρ are given in Table IV. The values of $\bar{\mu}_{\mathrm{Ni}}$ obtained by the two different fittings are in reasonable agreement (see Tables III and IV). The change of the moment disturbances produced by the high field for the 52.5% alloy scales approximately with the change of moment. A small decrease of Γ is also observed. In Table IV are also given the values of the first-shell perturbations $\phi_1(R_1)$ given by the magnetic environment model [Eq. (6.17)], and the "chemical environment" part of it $\rho\Gamma$. Most of the effect is due to the magnetic environment.

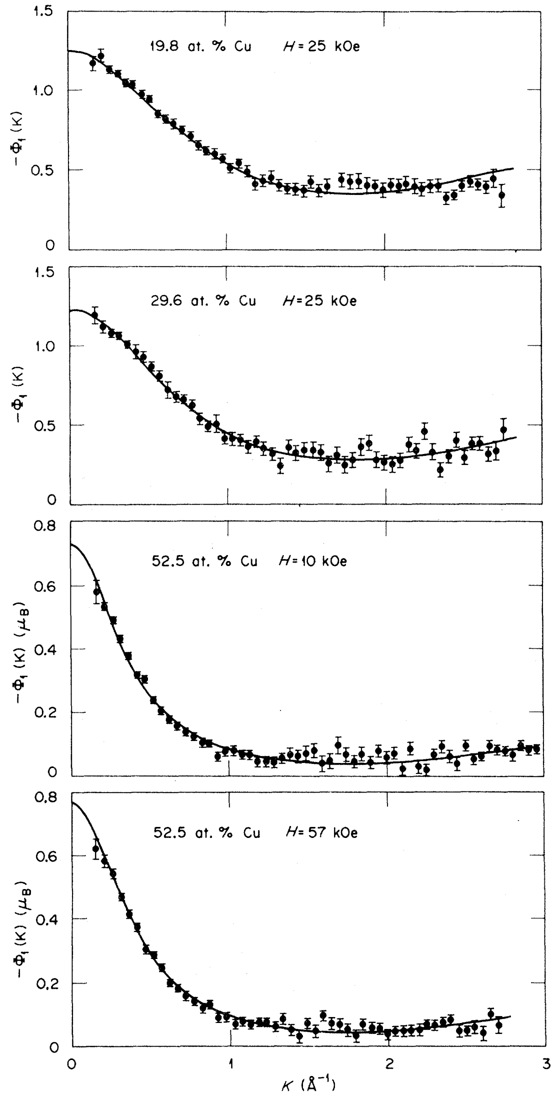

FIG. 4. Moment disturbances of random Ni-Cu alloys fitted with the magnetic-environment model.

TABLE III. Average Ni moments.

c	$\langle\mu_{\mathrm{Ni}}\rangle$	$\langle\mu_{\mathrm{Ni}}\rangle_{\mathrm{CAL}}$	$\bar{\mu}_{\mathrm{Ni}}$
0.198	0.478	0.481	0.466
0.296	0.413	0.414	0.382
0.525	0.091	0.090	0.0765
0.525 (HF)[a]	0.106	0.106	0.0776

[a] HF, high field.

TABLE IV. Fitting of the magnetic-environment model.

c	$\bar{\mu}_{\mathrm{Ni}}$	Γ	ρ	χ^2/N	$\phi_1(R_1)$	$\rho\Gamma$
0.198	0.461 (6)	0.515 (34)	−0.027 (8)	1.23	−0.0427	−0.0139
0.296	0.379 (8)	0.583 (36)	−0.023 (7)	1.15	−0.0424	−0.0135
0.525	0.0713 (29)	0.871 (10)	−0.0034 (7)	1.41	−0.0146	−0.0029
0.525 (HF)[a]	0.0776 (26)	0.856 (9)	−0.0046 (6)	0.98	−0.0167	−0.0039

[a] HF, high field.

B. Response function

We now present a semiphenomenological determination of the response function $F(h, \nu, c)$ that appears in the magnetic environment model. Our purpose is not to give an exact calculation of $F(h, \nu, c)$, but rather to illustrate the behavior of the model. We start by considering the pure-Ni case. Cooke and Davis[32] have calculated the bands of ferromagnetic Ni using the paramagnetic band structure of Stocks *et al.*[8] Their band calculation shows a $\vec{K}$-dependent exchange splitting. However, the integrated density of states they obtain can be approximately described with a different rigid splitting for each one of the t_{2g}, e_g, and sp densities of states. We use the Stocks *et al.* densities of states of paramagnetic Ni for estimating the spin moment as a function of the t_{2g} band half-splitting I. A variety of splitting schemes were tried and they yield different values between 0.0135 and 0.0160 Ry for the splitting, I_0, which reproduces the observed spin moment (0.56 μ_B). However, all of them give almost identical results when the spin moment is plotted against I/I_0. This plot is given in Fig. 5. We assume that this function applies locally to each Ni atom, and that the splitting I is linearly dependent on the moment of the atom itself and on those of the nearest neighbors. We then write the splitting of the atom at site $\vec{r}$ as

$$I_{\vec{r}} = j_0 \mu_{\vec{r}} + j_1 \sum_{\vec{\delta}} \mu_{\vec{r}+\vec{\delta}} = j_0 \mu_{\vec{r}} + h(\vec{r}) , \tag{7.1}$$

where j_0 is the intra-atomic and j_1 is the interatomic exchange parameter.

We consider now the Ni-Cu case. We use the same procedure to determine the spin moment as a function of splitting for different Cu concentrations, using the Ni densities of states given by the CPA calculations of Ref. 8. The moment-versus-splitting curves so obtained are roughly proportional to the pure-Ni curve. However, the decrease of moment predicted using these curves is too large: the predicted critical concentration is less than 40-at.% Cu. Instead of using those functions we assume the following phenomenological formula for the moment of a Ni atom at site $\vec{r}$ and surrounded by ν Cu atoms:

$$\mu_{\vec{r}} = (1 - \beta\nu)(\tfrac{1}{2}g) f(I_{\vec{r}}) . \tag{7.2}$$

Here, $I_{\vec{r}}$ is given by Eq. (7.1), β is a parameter that measures the strength of the "chemical environment effect," and $f(I)$ is the spin moment for a splitting I in pure Ni. Equations (7.2) and (7.1) give an implicit definition of the response function $F(h, \nu)$. The explicit c dependence is neglected. Equations (7.2) and (6.14) give the following expressions for ρ:

$$\rho = -\frac{\beta}{1 - 12c\beta} \, \frac{\bar{\mu}}{1 - (1 - 12c\beta)(\frac{1}{2}g)(df/dI)j_0} \, \frac{1}{\Gamma} , \tag{7.3}$$

and for Γ at zero-impurity concentration

$$\Gamma_0 = \frac{12 j_1 (\frac{1}{2}g)(df/dI)}{1 - (\frac{1}{2}g)(df/dI) j_0} . \tag{7.4}$$

So far we have two unknown parameters, β and α, the fraction of the splitting that is due to interatomic exchange, i.e.,

$$\alpha = 12 j_1 / (j_0 + 12 j_1) . \tag{7.5}$$

The self-consistent method explained in Sec. VI gives Γ and $\bar{\mu}$ as a function of Cu content for any

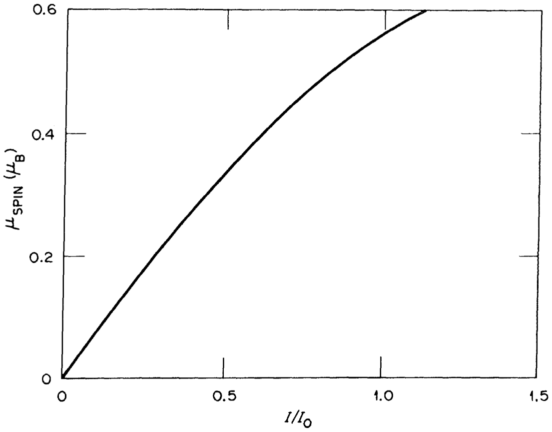

FIG. 5. Spin moment of Ni as a function of the relative band splitting.

given $F(h, \nu, c)$. We use this fact to determine the values of α and β that reproduce the magnetization data. In doing this, we take into account the random-alloy assumption by calculating, with Eq. (5.6), the moment in the presence of clustering. In the calculation only $\alpha(R_1)$ was assumed nonzero. We find the intervals $0.20 < \alpha < 0.40$, $0.01 < \beta < 0.02$ for the parameters. The values $\alpha = 0.32$ and $\beta = 0.0154$ give the best agreement with the cross sections. The average moment calculated using these values is shown in Fig. 6, while Γ and ρ are given in Fig. 7 together with the experimental values. The 10- and 40-at.%-Cu unpolarized-neutron data of Aldred *et al.*[2] are compared with the predicted cross sections in Fig. 8. We see that this very simple model gives the right trend of the cross sections. Some difference is to be expected in the 40% alloy because of the problems of the unpolarized neutron data already discussed in Sec. III. We do not expect the model to properly describe the critical region, because it completely neglects the appearance of uncoupled superparamagnetic clusters which are polarized when a magnetic field is applied. It has been implicitly assumed instead that all the moments are aligned. The predicted critical concentration is 60-at.% Cu ($\Gamma \sim 1$) which agrees more with the concentration at which the Curie-Weiss interaction temperature goes negative[33] than with the observed critical concentration of 57-at.% Cu. The difficulties in the critical region are due to the particular solution and not to the magnetic environment model itself, which can actually be used for estimating the stability of clusters and their moments in the paramagnetic alloys.

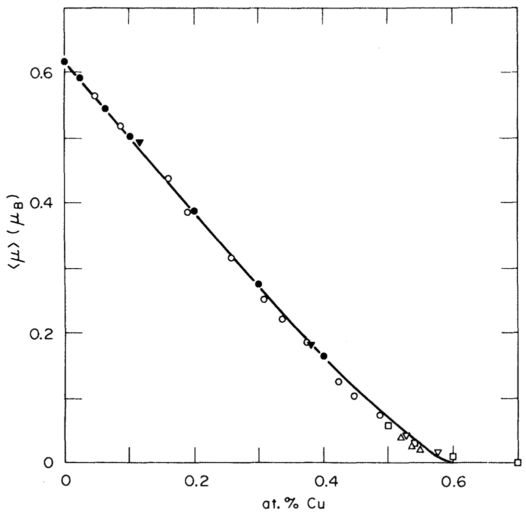

FIG. 6. Data and theoretical calculations of the Ni-Cu average moment. ▼, Ref. 9; ○, Ref. 19 (normalized to a pure-Ni moment of $0.616\mu_B$); ●, Ref. 2; △, Ref. 20; ▽, Ref. 21; □, Ref. 22.

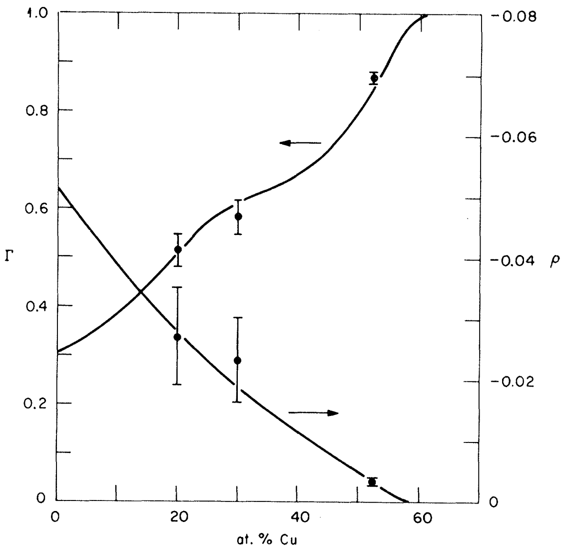

FIG. 7. Experimental and theoretical values of the parameters Γ and ρ of the magnetic environment model.

A better and less phenomenological determination of $F(h, \nu, c)$ is needed for a better understanding of the Ni-Cu systems.

C. Dilute impurities

The value of Γ at zero concentration Γ_0 is a property of pure Ni. We should therefore expect

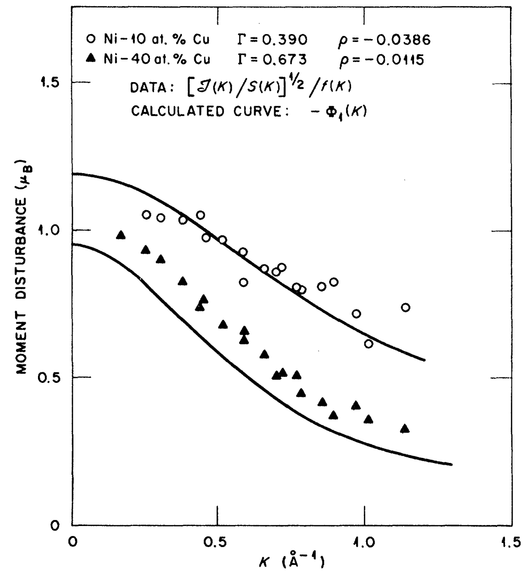

FIG. 8. Ni-Cu unpolarized-neutron moment disturbances from Ref. 2 compared with the predictions of the magnetic-environment model.

that any dilute nonmagnetic impurity produces a moment disturbance $\Phi_1(\vec{K})$ described by Eq. (6.25) with Γ equal to Γ_0, and a ρ that depends on the strength of the "chemical perturbation." The value of Γ_0, calculated with the chosen parameters α and β, is $\Gamma_0 = 0.305 \pm 0.05$. Using this value we have calculated ρ in the dilute limit for different nonmagnetic impurities by equating $d\langle\mu\rangle/dc$ with $\Phi_1(0)$. When no derivative value was available we used a $\Phi_1(0)$ value calculated from the data of Ref. 25. The results of this calculation are plotted in Fig. 9, and show an increase of the chemical disturbance as the atomic number of the impurity moves away from Ni. As an example, we present in Fig. 10 the Ni-1-at.%-Cr polarized-neutron data of Cable and Medina,[34] and the *Ni*-Zn data of Comly *et al.*[25] together with the predicted moment disturbances. The agreement of predicted and measured moment disturbances of impurities as different as Zn and Cr indicates that the Γ_0 estimated is not far from the actual value. We should note that the present model, in contrast with the one proposed by Comly *et al.*,[25] does not predict a universal moment disturbance; the shape of the moment disturbance is instead ρ dependent. For example, Zn was considered to be anomalous because of the shorter range of its moment disturbance, but this is given correctly by the present model. Their qualitative discussion of the moment perturbation induced by an impurity on its Ni neighbors and its propagation through the nickel matrix is, however, also applicable to our model.

VIII. SUMMARY AND CONCLUSIONS

We have measured the moment disturbances in three ferromagnetic Ni-Cu alloys with the polarized-neutron technique. The data indicate that all the magnetic moment, including the negative magnetization previously assumed uniform, is to be associated with the Ni atoms. This agrees with the diffraction data,[9] and with the theoretical[7,8] and experimental[5,6] evidence that the Cu atoms keep their 3*d* shell almost full.

The proposed nearest-neighbor magnetic-environment model gives an excellent description of the observed moment disturbances. Within the model one finds that most of the moment disturbances produced by Cu in Ni are due to its nonmagnetic character, but that some nearest-neighbor chemical disturbance must be included to explain the observed cross sections. In contrast, none of the first- and second-shell chemical-environment models, like those of Refs. 9, 21, 22, and 35, is consistent with the diffuse-scattering data. The proposed model also describes the diffuse scattering of other nonmagnetic dilute impurities in Ni, because the moment disturbance induced by the impurity in its Ni neighbors is propagated through the lattice with the same mechanism, regardless of the origin and size of the disturbance.

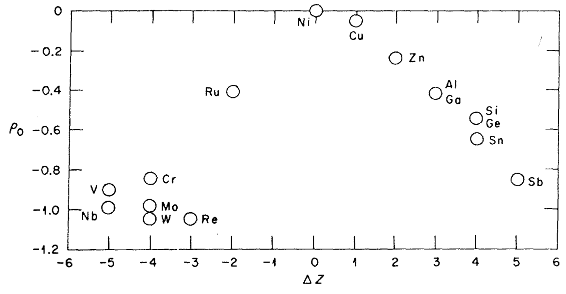

FIG. 9. Chemical disturbance parameter ρ for different diluents in Ni as a function of the charge contrast.

The large and long-range moment disturbances produced by impurities suggest that some type of effective interatomic exchange is very important for Ni. A rough Stoner type of calculation shows that between 20% and 40% interatomic exchange is needed to reproduce the Ni-Cu data. Within the same calculation each Cu atom induces a (1–2)% moment reduction on its Ni neighbors for any given exchange field. For a better determination and understanding of these effects, a more accurate and less phenomenological calculation should be performed. However, our data indicates that, independent of the specific model used to describe magnetic cooperative effects, such effects are dominant in determining the magnetic moments in Ni-Cu alloys.

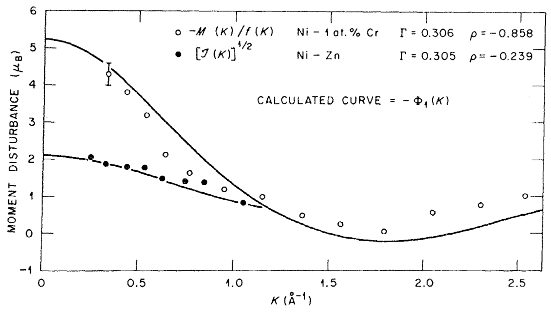

FIG. 10. *Ni*-Cr (1-at.%) polarized-neutron data of Ref. 33 and *Ni*-Zn [between (2 and 4)%] unpolarized-neutron data of Ref. 25 compared with the theoretical predictions.

ACKNOWLEDGMENTS

We would like to express our appreciation to B. Mozer for loaning us the alloys used in this study, and to J. F. Cooke and J. S. Faulkner for providing us with the Ni and Ni-Cu densities of states. We also thank T. Kaplan, M. Mostoller, R. M. Moon, J. W. Garland, and A. Gonis for very useful discussions, and H. R. Child and J. L. Sellers for assistance in the experiment.

---

*Research sponsored by the U.S. Energy Research and Development Administration under contract with Union Carbide Corp.

†Present address: Instituto Venezolano da Investigaciones Cientificas, Caracas, Venezuela.

[1] J. W. Cable, E. O. Wollan, and H. R. Child, Phys. Rev. Lett. 22, 1256 (1969).

[2] A. T. Aldred, B. D. Rainford, T. J. Hicks, and J. S. Kouvel, Phys. Rev. B 7, 218 (1973).

[3] W. Marshall, J. Phys. C 1, 88 (1968).

[4] H. A. Mook, Phys. Rev. 148, 495 (1966).

[5] D. H. Seib and W. E. Spicer, Phys. Rev. B 2, 1676 (1970); 2, 1694 (1970).

[6] S. Hüfner, G. K. Wertheim, R. L. Cohen, and J. H. Wernick, Phys. Rev. Lett. 28, 488 (1972).

[7] S. Kirkpatrick, B. Velicky, and H. Ehrenreich, Phys. Rev. B 1, 3520 (1970).

[8] G. M. Stocks, R. W. Williams, and J. S. Faulkner, Phys. Rev. B 4, 4390 (1971).

[9] Y. Ito and J. Akimitsu, J. Phys. Soc. Jpn. 35, 1000 (1973).

[10] J. W. Garland and A. Gonis, in *Magnetism in Alloys*, edited by P. A. Beck and J. T. Waber (AIME, New York, 1972), p. 79.

[11] R. A. Medina and J. W. Garland (unpublished).

[12] In a preliminary report of the data the value 53.5% was used. R. A. Medina and J. W. Cable, AIP Conf. Proc. 29, 292 (1976).

[13] M. Hayase, M. Shiga and Y. Nakamura, J. Phys. Soc. Jpn. 34, 925 (1973).

[14] B. N. Brockhouse, L. M. Corliss, and J. M. Hastings, Phys. Rev. 98, 1721 (1955).

[15] J. Schelten and F. Hossfeld, J. Appl. Crystallogr. 4, 210 (1971).

[16] B. Mozer, D. T. Keating, and S. C. Moss, Phys. Rev. 175, 868 (1968).

[17] G. P. Flecher, J. W. Garland, J. W. Cable, and R. Medina, AIP Conf. Proc. 29, 331 (1976).

[18] R. M. Moon, AIR Conf. Proc. 24, 925 (1975).

[19] S. A. Ahern, M. J. C. Martin, and W. A. Sucksmith, Proc. R. Soc. A 248, 145 (1958).

[20] C. G. Robbins, H. Claus, and P. A. Beck, J. Appl. Phys. 40, 2269 (1969).

[21] J. P. Perrier, B. Tissier, and R. Tournier, Phys. Rev. Lett. 24, 313 (1970).

[22] S. Mishra, Int. J. Magn. 5, 363 (1974).

[23] F. Acker and R. Huguenin, Phys. Lett. A 38, 343 (1972).

[24] E. Balcar and W. Marshall, J. Phys. C 1, 966 (1968).

[25] J. B. Comly, T. M. Holden, and G. G. Low, J. Phys. C 1, 458 (1968).

[26] L. M. Roth, Phys. Rev. B 2, 740 (1970).

[27] H. Dvey-Aharon and M. Fibich, Phys. Rev. B 10, 287 (1974).

[28] J. W. Garland, A. Gonis, J. S. Kouvel, and A. T. Aldred, AIP Conf. Proc. 10, 1638 (1972).

[29] T. J. Hicks, Phys. Lett. A 32, 410 (1970).

[30] S. W. Lovesey and W. Marshall, Proc. Phys. Soc. Lond. 89, 613 (1966).

[31] G. S. Joyce, J. Phys. C 4, 153 (1971).

[32] J. F. Cooke and H. L. Davis, AIP Conf. Proc. 10, 1218 (1973).

[33] J. S. Kouvel and J. B. Comly, Phys. Rev. Lett. 24, 598 (1970).

[34] J. W. Cable and R. A. Medina, Phys. Rev. B 13, 4868 (1976).

[35] C. G. Robbins, H. Claus, and P. A. Beck, Phys. Rev. Lett. 22, 1307 (1969).